

T. Haslwanter · R. Jaeger · S. Mayr · M. Fetter

## Three-dimensional eye-movement responses to off-vertical axis rotations in humans

Received: 30 August 1999 / Accepted: 17 March 2000 / Published online: 28 June 2000  
© Springer-Verlag 2000

**Abstract** We recorded three-dimensional eye movements elicited by velocity steps about axes that were tilted with respect to the earth-vertical. Subjects were accelerated in 1 s from zero to 100°/s, and the axis of rotation was tilted by 15°, 30°, 60°, or 90°. This stimulus induced a constant horizontal velocity component that was directed *opposite* to the direction of rotation, as well as a modulation of the horizontal, vertical and torsional components with the frequency of the rotation. The maximum steady-state response in the horizontal constant-velocity component was much smaller than in other species (about 6°/s), reaching a maximum at a tilt angle of about 60°. While the amplitude of the horizontal modulation component increased up to a tilt angle of 90° (8.4°/s), the vertical and torsional modulation amplitudes saturated around 60° (ca. 2.5°/s). At small tilt angles, the horizontal modulation component showed a small phase lag with respect to the chair position, which turned into a small phase lead at large tilt angles. The torsional component showed a phase lead that increased with increasing tilt angle. The vertical and torsional velocity modulation at large tilt angles was not predicted by a recent model of otolith-canal interaction by Merfeld. Agreement between model and experimental data could be achieved, however, by introducing a constant force along the body's z-axis to compensate for the gravitational pull on the otoliths in the head-upright position. This approach had been suggested previously to explain the direction of the perceived subjective vertical during roll under different g-levels, and produced in our model the observed vertical and torsional modulation components at large tilt angles.

**Key words** Off-vertical axis rotation · Three-dimensional eye movements · Multisensory integration · Otolith-canal interaction · Modeling · Human

### Introduction

The vestibular system is the dominant source of information for our perception of orientation and movement in space. The importance of this system becomes obvious during an acute loss of this input, which causes severe difficulties during movements of the head. The vestibular system consists of two components that cooperate to indicate our orientation and movement in space: the otoliths and the semicircular canals. The semicircular canals transduce only rotational movements and respond only to acceleration and deceleration, but not to constant-velocity rotations. The otoliths, in contrast, are responsible for the determination of our orientation with respect to gravity and for the transduction of linear acceleration.

The otolith signals interact with signals from the semicircular canals to generate a combined eye-movement command. Studies of three-dimensional eye movements have revealed that in monkeys static otolith inputs lead to a strong interaction of horizontal, vertical, and torsional eye-movement components (Angelaki and Hess 1994; Merfeld and Young 1995). Human responses, in contrast, are influenced much less by such static otolith inputs (Fetter et al. 1996; Curthoys et al. 1998). While the effects of dynamic otolith-canal interaction on horizontal, vertical, and torsional eye movements have been investigated in other species, no such study exists for human subjects. Below we present the results of the first such study, which was done by recording three-dimensional eye movements during rotations about an off-vertical axis (OVAR) tilted by varying amounts with respect to gravity. During and immediately after the acceleration and deceleration, the semicircular canals and the otoliths are stimulated simultaneously, and their combined input is used to estimate the orientation and move-

T. Haslwanter  
Department of Neurology, Frauenklinikstrasse 26,  
CH-8091 Zurich, Switzerland

T. Haslwanter  
Department of Neurology,  
University Hospital Zurich and Institute of Theoretical Physics,  
ETH Zurich, Switzerland

R. Jaeger · S. Mayr · M. Fetter  
Department of Neurology, Tübingen University, Germany

ment in space. In the steady state only the otoliths generate an input, while the semicircular canals indicate no rotation.

During OVAR, cats (Harris 1987; Darlot and Denise 1988), monkeys (Raphan et al. 1981; Angelaki and Hess 1996a), and rats (Hess and Dieringer 1990) generate steady state eye movements that compensate well for the movement of the body in space. The response in humans, however, seems to be different: the few studies that have investigated the eye movements elicited by OVAR indicate that this stimulus induces only a small horizontal eye-movement response (Harris and Barnes 1987; Furman et al. 1992; Darlot et al. 1988).

The interaction of otolith input with canal-induced signals in three dimensions is quite complex, and a purely intuitive interpretation of the results often fails. Therefore we used a model-based approach to gain a better understanding of the signal processing during OVAR. Most models describing OVAR deal exclusively with dynamic otolith stimulation (Hain 1986; Schnabolk and Raphan 1992; Hess 1992; Angelaki 1992a, 1992b). One model combines information from the canals and otoliths but is quite specific for the stimulation during postrotatory tilt (Angelaki and Hess 1995a). Only the models by Merfeld et al. (1993) and a very similar one by Glasauer (Glasauer and Merfeld 1997) describe the interaction of canals and otoliths in three dimensions for arbitrary movements in space. The model by Merfeld has recently been used successfully to explain eye movement characteristics after postrotatory tilts, which could not be understood by considering only the instantaneous inputs to the vestibulo-ocular system (Merfeld et al. 1999). We therefore based our modeling approach on Merfeld's studies.

## Materials and methods

### Experimental setup

Subjects were seated inside an opaque sphere with a diameter of 1.9 m and were firmly secured to the chair with seat belts. They were positioned such that the center of the interaural line was at the center of rotation.

To fixate the body, deflatable vacuum cushions were used which adjust themselves to the shape of the body. The head was in a comfortable, upright position, and head movements were minimized by a helmet and an attached bite-bar.

### Eye position recording

Three-dimensional eye position was recorded with the dual search-coil technique, using the commonly employed Skalar search coils (Skalar, Delft, Netherlands). The magnetic field was produced by three orthogonal pairs of coils, with a diameter and a separation of 1.4 m, and was such that the head of the subject was at the center of the magnetic fields. Signals from all three fields were recorded, and the system was calibrated automatically at the beginning of the experiments. Data were sampled at 100 Hz, and the reference position was taken from the beginning or the end of the experimental session, when the subject was looking straight ahead. The automatic calibration procedure, as well as technical details of the data acquisition, are described in Bechert and Koenig (1996).

### Paradigms

OVAR is a highly nauseous stimulus, and it is difficult to test a large number of parameters within one single subject. Therefore we used two subject groups. All subjects were healthy and had no prior history of vertigo or dizziness. Group I was made up of 11 individuals, aged  $24 \pm 2.4$  years (mean  $\pm$  SD). Group II contained five subjects, aged  $26.2 \pm 5.6$  years. All subjects gave informed consent to the recordings, which were performed in accordance with protocols approved by the institutional ethics committee. They were asked to keep the head in a comfortable, upright position, with Reid's line about  $8^\circ$  nose up, and the helmet was locked in that position. Apart from the fixation of a set of horizontal or vertical calibration points within the range of  $15^\circ$  at the beginning and at the end of each recording, the experiments were performed in complete darkness, and subjects were instructed to keep on looking straight ahead throughout the experiment. Following an initial calibration, the whole setup was pitched backwards about the interaural axis of the subject, so that the subject was in a supine position. After a few seconds in this position, they were accelerated about the tilted yaw axis at  $100^\circ/\text{s}^2$  to a constant velocity of  $100^\circ/\text{s}$ . The direction of the first acceleration was varied randomly. After a constant-velocity rotation of about 60 s, subjects were decelerated at  $100^\circ/\text{s}^2$ . The deceleration was timed such that they ended up in the supine starting position. When the postrotatory nystagmus was finished, the experiment was repeated in the *opposite* direction. Then the tilt angle of the whole setup was changed and OVARs were again repeated in both directions. In group I we recorded the responses to rotations about an earth-vertical axis and about an axis that was tilted first by  $15^\circ$  and then by  $30^\circ$ . In group II the tilt angle was randomly varied between  $30^\circ$ ,  $60^\circ$ , and  $90^\circ$ .

To complement our study with data from rotations at higher velocities, we reanalyzed data recorded previously by Tweed et al. (1994). They had tested subjects during earth-horizontal axis rotation at  $150^\circ/\text{s}$  but had analyzed only the initial part of the response.

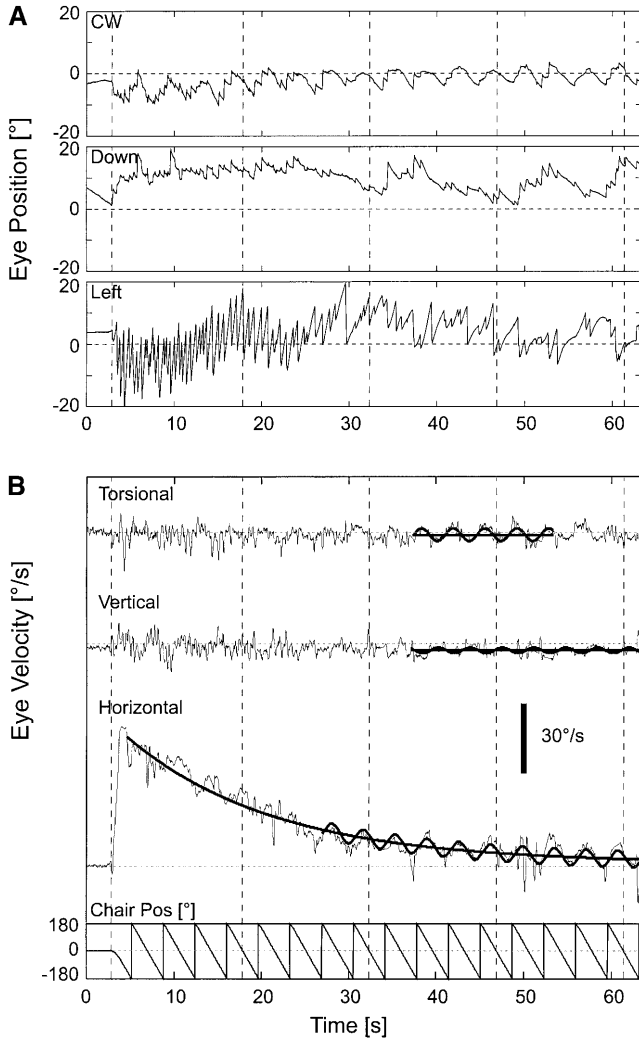
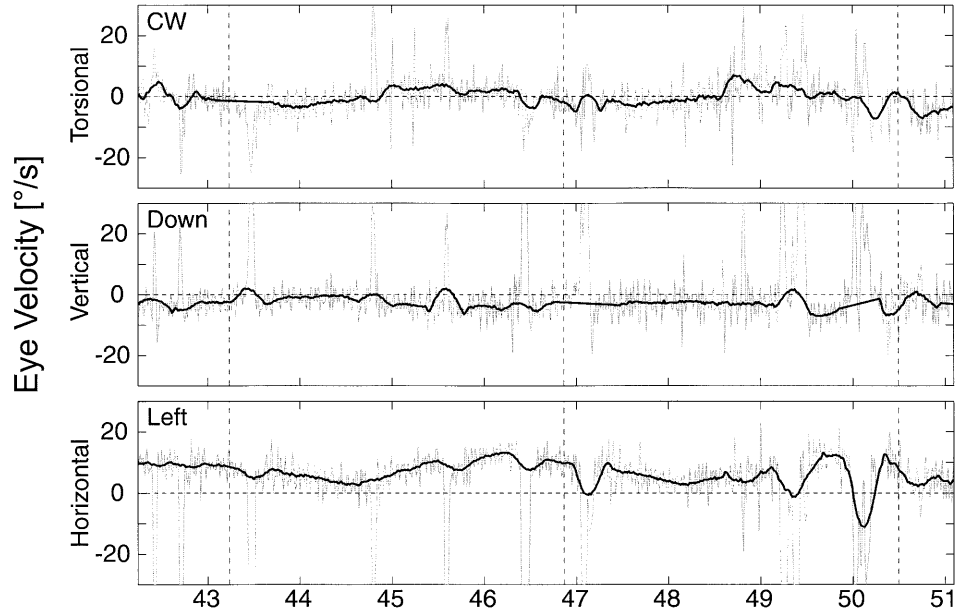
### Data analysis

The recorded three-dimensional eye and head positions were converted to quaternions, with the reference position chosen as described above. The terms *horizontal*, *vertical*, and *torsional* refer to the movement of the eye with respect to a head-fixed coordinate system, which is rotating with the subject and determined by the orientation of the magnetic fields. Eye movements to the left, down, and clockwise (as seen from the subject) are positive. The time derivative of the eye position was calculated with a Savitzky-Golay filter (Savitzky and Golay 1964; Press et al. 1992): a 2nd-order polynomial was used, and five samples before and after the current point were taken into consideration. From the eye position and this time derivative, three-dimensional eye velocity was calculated (Tweed et al. 1990). Nystagmus fast phases were removed with an algorithm developed by Holden (Holden et al. 1992), and start- and end-points of each fast phase were linearly connected. The data were smoothed before further analysis (again with a Savitzky-Golay filter, with 15 points before and after each sample). A superposition of the original eye-velocity traces with the desaccaded data is shown in Fig. 1. Since our data fits were always over a number of cycles (see Fig. 2), the small artifacts occasionally introduced by the interpolation of the saccadic intervals should have a negligible effect on the fits.

In the few cases where this procedure could not eliminate most saccades, the fast phases of the nystagmus were removed by grouping data into bins of 100 data points each and calculating the median for each bin. Neighboring bins were overlapping, staggered by five data points. This produced a coarser result but a more thorough desaccading. Visual inspection of the original eye-velocity data superposed with the desaccaded data ensured proper desaccading.

A typical eye-velocity response to OVAR is shown in Fig. 2. At first sight the eye velocity traces appear very "noisy" (Fig. 2B).

**Fig. 1** Rotations about an off-vertical axis at 100°/s about an axis tilted 30° with respect to gravity: torsional, vertical, and horizontal eye-velocity responses (*thin gray lines*), and corresponding desaccaded data traces (*thick black lines*). The desaccaded data correspond to the data in Fig. 2B. *Dashed vertical lines* mark each zero chair position



But a look at Fig. 1 confirms that the bigger variations in the desaccaded eye-velocity traces (e.g., at 50 s) do in fact correspond to variations in the original eye-velocity data.

The horizontal eye-velocity response consists of a sinusoidal modulation on top of an exponential decay to a constant velocity (Fig. 2B). The desaccaded horizontal eye-velocity traces were used to find the maximum eye velocity. To determine the time constant of the subsequent exponential decay, data were fit with a single exponential, allowing for a decay to a nonzero steady state velocity. We are going to call the constant velocity indicated by the fit as *offset*, in order to distinguish it from the established term *bias*, used for the difference between the response about an earth-vertical axis and a tilted axis. Because of the nauseous nature of the stimulus, the rotations had to be kept short (ca. 60 s), and the eye velocity could not always reach the steady state completely. For consistency, the same time period was used in the analysis of rotations about an earth-vertical axis. This had the effect that at the end of our analysis interval (60 s) the eye velocity elicited by a rotation about an earth-vertical axis is frequently in the direction of the rotation, i.e., *opposite* to the initial eye-movement direction, because of an adaptation phenomenon sometimes referred to as “secondary nystagmus.” For such earth-vertical axis rotations, the offset was 2.2°/s (Table 1), but the bias is, by definition, zero.

For the vertical and torsional directions, the velocity offsets were determined by averaging the desaccaded velocity traces over a hand-selected interval toward the end of the recording. Manual selection of the fitting interval ensured that natural variations in the eye velocity traces (e.g., the variations in the horizontal eye-velocity trace at 50 s in Fig. 2B) did not distort the fitted data.

The amplitude and phase of the sinusoidal modulation of eye velocity was calculated by fitting the function: eye velocity = amplitude × sin(φ + Δφ) to a hand-selected interval of the eye velocity traces, after the exponential decay and the offset were subtracted.

**Fig. 2** **A** Torsional, vertical, and horizontal eye position during rotations about an off-vertical axis at 100°/s about an axis tilted 30° with respect to gravity. **B** Corresponding eye velocities. The *bottom panel* gives the chair position in degrees, with 0° the nose-up position. *Dashed vertical lines* mark every 4th zero-position of the chair. The *thick solid lines* superposed on the eye velocity traces indicate the fitted data and the range chosen for the fit

**Table 1** Mean values and standard deviations of offset, modulation amplitude, and modulation phase of the eye velocity during rotation at 100°/s about a yaw axis tilted with respect to the verti-

cal. For the offset and the amplitude, the values for each subject have been averaged for rotations to the right and the left so that the offset values correspond to a rotation to the right

HVT	Tilt (°)	Offset (°/s)		Amplitude (°/s)		Phase (°)			
		Mean±SD	Subjects ( <i>n</i> )	Mean±SD	Subjects ( <i>n</i> )	Right		Left	
						Mean±SD	Subjects ( <i>n</i> )	Mean±SD	Subjects ( <i>n</i> )
Horizontal	0	-2.2±1.4	10						
	15	0.1±1.5**	10	1.6±0.8	10	-17.1±25	9	-13.1±20	8
	30	2.0±1.4**	12	3.5±0.9**	12	-12.6±22	10	-9.9±28	12
	60	4.0±2.6***	5	7.2±1.7**	5	3.9±12	4	14.6±23	4
	90	3.9±4.8	4	8.4±2.7	4	6.1±23	3	18.1±22	4
Vertical	15	-0.3±1.6	10	1.2±0.5	10	-154.0±12	5	46.6±23	3
	30	-0.4±1.9	12	1.8±0.8*	12	-141.9±36	10	32.8±35	9
	60	-1.8±5.1	5	2.8±1.5	5	-108.5±98	4	62.1±66	3
	90	0.2±2.8	4	2.6±1.5	4	-130.7±52	3	-2.7±22	3
Torsional	15	-0.1±0.3	10	1.1±0.4	10	14.6±8	6	7.4±14	5
	30	0.0±0.9	12	1.9±0.8**	12	23.3±16	10	26.5±22	10
	60	-1.2±3.6	5	2.4±0.9	5	23.3±26	4	52.8±16	4
	90	-0.9±1.1	4	2.5±0.4	4	78.6±20	2	133.5±66	4

Statistical differences to the corresponding value for the next-smaller tilt angle: \* $P<0.05$ ; \*\* $P<0.01$

\*\*\*A statistical difference only on a paired  $t$ -test ( $n=2$ )

$\phi$  is the phase of the horizontal chair position, with  $\phi=0$  when the subject is in the supine (nose-up) starting position.  $\Delta\phi$  is the phase difference between eye velocity and chair position.

Rotations to the right and to the left showed no significant difference. Therefore corresponding amplitude and offset values were averaged for each subject when data from rotations to the left and to the right were available. In doing so, the horizontal and torsional traces of data from leftward rotations were inverted so that all data corresponded to rotations to the right. The means and standard deviations for the group were calculated from these averaged values. To see if any of the parameters characterizing the eye movements changed as a function of the tilt angle, we performed paired  $t$ -tests when the same subjects were tested for different tilt angles, and unpaired  $t$ -tests otherwise. We used a significance criterion of  $P<0.05$ .

A different analysis was used for the phase values. When the amplitude of the eye velocity modulation was smaller than 1°, or when inspection of the fits revealed an unreliable value, the corresponding phase value was discarded. When phase values were available for rotations to the left and the right, we distinguished between a temporal and a spatial phase-shift. A spatial phase shift could be caused by a preferred response direction to the vestibular stimulus (Angelaki and Hess 1996b) and was determined by subtracting  $\Delta\phi$  for rotations to the left and right. As explained in Appendix A, the phases for the vertical traces thereby had to be shifted for rotations in one direction by 180°, to account for the change in the direction of the reference phase (the chair position). Our analysis indicated that there was no spatial phase-shift, and in the following we attribute all phase shifts to temporal shifts. The variability of interindividual responses was quantified by calculating the “dispersion” for the phase values. For the Results, we converted the dispersions to the corresponding standard deviation values, as described in Appendix B.

The definition of the phase values is complicated, especially for the vertical traces (see also Appendix A), and different reference positions are used in each study (Harris and Barnes 1987; Darlot et al. 1988). To avoid any additional complications, we have not averaged the phase values for rotations to the left and the right, but present these values separately.

## Results

During OVAR about the body yaw axis, horizontal, vertical, and torsional eye position traces were modulated. Typical eye position traces are shown in Fig. 2A. The corresponding velocity traces (Fig. 2B) show clear velocity modulations, especially for the horizontal and torsional components. For the horizontal eye velocity, this modulation was superimposed on an exponential decay, caused by the stepwise acceleration about the yaw axis.

The values for the velocity offset and modulation are given in Table 1. The horizontal velocity offset increased with increasing tilt angle up to a tilt of 60°. For the vertical and torsional component the velocity offset was not significantly different from zero.

The modulation amplitude for the horizontal eye velocity increased with increasing tilt angle, although the increase from a tilt angle of 60° to 90° was not statistically significant. For the vertical and torsional component, the velocity modulation saturated at tilt angles of about 60°.

The phase showed consistent behavior for the horizontal and the torsional component but was more variable for the vertical component. For the horizontal trace, the phase showed a small lag at lower tilt angles, which turned into a lead at larger tilt angles. The torsional component showed a phase lead that increased with increasing tilt angle (Fig. 3).

The maximum horizontal eye velocity elicited by acceleration was independent of the tilt angle (Table 2). For deceleration the maximum velocity decreased with increasing tilt angle, as did the corresponding time constant.

To obtain data for higher velocity rotations, we analyzed the per-rotatory response during rotation about an

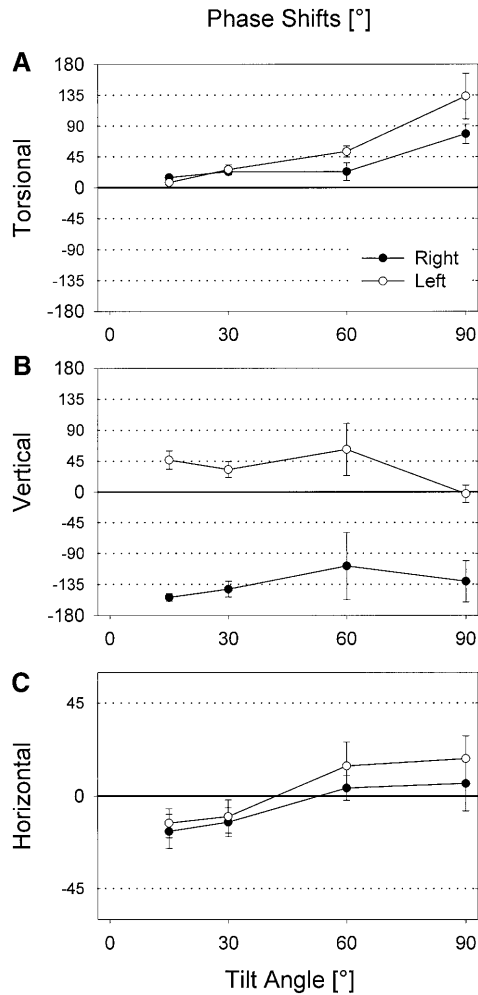


**Fig. 3A–C** Torsional (A), vertical (B), and horizontal (C) phase shifts for rotation to the left (empty circles) and right (full circles). Bars indicate standard errors. **B** For the vertical component the phases for rotations to the right and left side are shifted by 180°, as explained in Appendix A. **C** The scale for the horizontal phase shifts is increased to see the results more clearly

**Table 2** Maximum horizontal eye velocity (*MaxVel*), and the time constant (*Tc*) of the corresponding decay, for acceleration (*Acc*) and deceleration (*Dec*)

Tilt (°)	MaxVel (°/s)				Tc			
	Acc		Dec		Acc		Dec	
	Mean±SD	Subjects ( <i>n</i> )	Mean±SD	Subjects ( <i>n</i> )	Mean±SD	Subjects ( <i>n</i> )	Mean±SD	Subjects ( <i>n</i> )
0	49.5±11.8	10	-49.5±11.8	10	17.1±5.5	10	17.1±5.5	10
15	52.0±11.7	10	-46.9±8.9	10	11.8±3.4*	10	15.4±7.1	10
30	49.9±10.0	12	-39.8±7.3*	12	11.2±3.1	12	11.1±4.2	12
60	42.9±11.4	5	-42.0±2.6	5	17.4±5.8*	5	11.2±4.9	5
90	49.2±14.9	4	-41.2±7.5	4	13.7±3.2	4	8.3±3.3	4

Statistical difference to the corresponding value for the next-smaller tilt angle: \* $P < 0.05$

**Table 3** Parameters characterizing the three-dimensional eye velocity during yaw rotations about an earth-horizontal axis at 150°/s. The data were taken from earlier experiments performed on six subjects (Tweed et al. 1994)

Tilt (deg)	Offset (°/s)		Amplitude (°/s)		Phase (deg)	
	Mean±SD	Subjects ( <i>n</i> )	Mean±SD	Subjects ( <i>n</i> )	Mean±SD	Subjects ( <i>n</i> )
Horizontal	5.9±6.3	5	8.6±4.1	6	-2±14	6
Vertical	-5.1±4.2	6	4.8±3.0	6	35±40	5
Torsional	0.5±1.3	6	3.7±1.4	6	-5±54	5

earth-horizontal axis (i.e., at a tilt angle of 90°) at 150°/s (Table 3). These experiments had been done by Tweed et al. (1994), but their analysis concentrated on the responses during the acceleration phase. Our analysis of these data indicates a further, although statistically insignificant increase in the horizontal offset and modulation amplitude, as well as in the vertical and torsional modulation amplitudes. We also found a significant negative vertical eye-velocity component ( $P < 0.035$ ).

## Modeling

Using SIMULINK and MATLAB (The MathWorks, Natick, Mass., USA), we implemented a model of otolith-canal interaction. The basic structure of the model is equivalent to the one suggested by Merfeld (1995; Merfeld et al. 1993), and is shown in Fig. 4. Details of the model have been presented previously (Merfeld et al. 1995a) and are summarized in Appendix C.

An implementation of the original model by Merfeld confirmed that the model predictions agree well with the experimental results for small angles of tilt. For tilt angles larger than 45°, however, the model predicted decreasing vertical and torsional eye-velocity modulations, with no vertical or torsional modulations at all for rotations about an earth-horizontal axis. As can be seen clearly in Fig. 5, this feature of the model disagrees with our experimental results. To bring the predictions of the model into agreement with the experimental data, we therefore had to modify and extend the model. In Fig. 4 the modified elements are indicated by a black shadow.

To reproduce the vertical and torsional eye-velocity modulation components found during OVAR at large tilt angles, we followed a suggestion by Dai et al. and modified the otolith transfer functions  $S_{oto}$ , given simply by the identity matrix in the original model (Dai et al. 1989). Physiologically a unity otolith transfer function

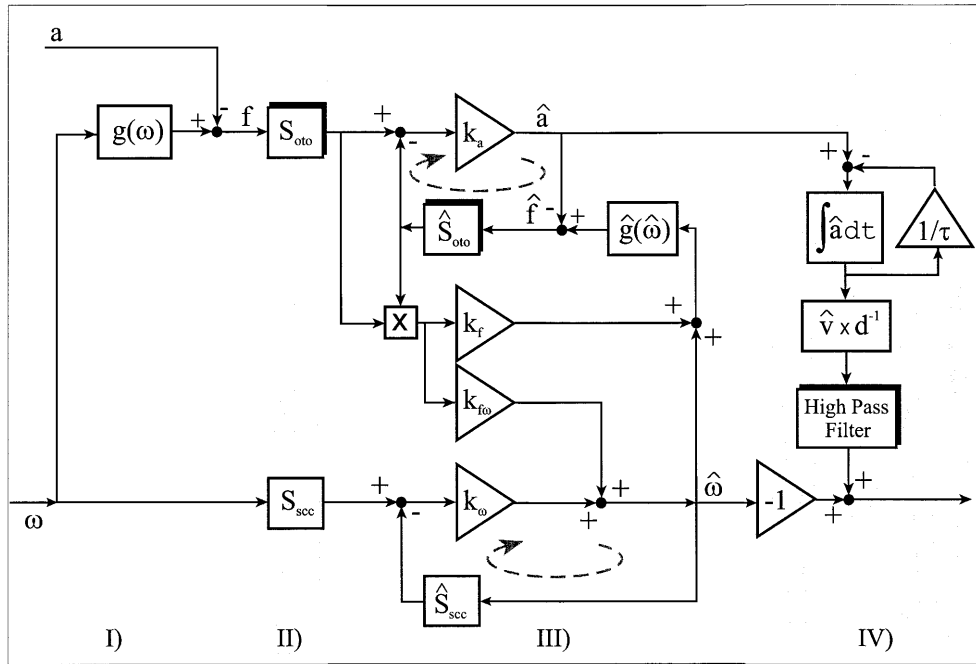


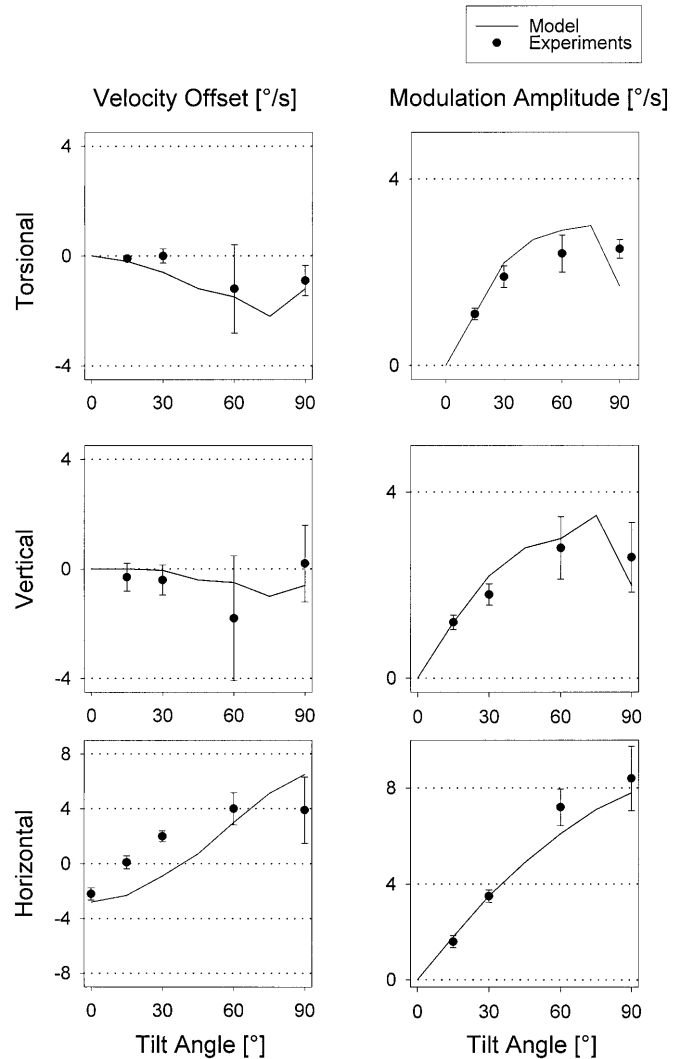
**Fig. 4** Model of otolith-canal interaction, adapted from Merfeld (1995). Elements that have been changed with respect to the original model have a *black shadow*. From left to right, the panels represent: movement in space (I), transduction by otoliths and canals (II), internal processing (III), vestibulo-ocular reflex (IV):

$$S_{scc} = \frac{\tau_d S}{\tau_d S + 1} \frac{\tau_a S}{\tau_a S + 1}; \hat{S}_{scc} = \frac{\tau_d S}{\tau_d S + 1}$$

that best reproduce the experimental data are given in Appendix C. ( $\omega$  Angular velocity vector;  $a$  linear velocity vector;  $g(\omega)$  update of the current direction of gravity, based on the formula  $dg/dt = g \times \omega$ ;  $S_{scc}$  transfer function of the semicircular canals;  $S_{oto}$  transfer function of the otoliths, including a constant pitch-shear force component along the utricular plane;  $x$  vector cross-product;  $k_r$  gain factors;  $\tau$  time constant of the leaky integrator;  $v$  linear velocity;  $d^{-1}$  inverse gaze direction;  $\hat{\cdot}$  estimated values, e.g.,  $\hat{\omega}$  is the estimated angular velocity)

corresponds to perfect force transduction by the otoliths. Dai speculated that an elastic restoring force may be acting on the otoliths to keep them in an equilibrium position when the head is upright. As the utricular plane and the angle of the saccular striola relative to the horizontal plane is oriented approximately  $30^\circ$  nose up in the normal head-upright position, the otoliths will be pulled backwards and downwards. To compensate for the gravitational pull, we therefore added a constant-force component along the  $z$ -axis to the otolith transfer function. The introduction of this element generated the required vertical and torsional velocity modulations during rotation about an earth-horizontal axis. Note that adding a constant external force to the otolith transfer function is

**Fig. 5** Torsional, vertical, and horizontal velocity offsets (left) and modulation amplitudes (right) of the eye velocity (degrees per second) during yaw-OVAR at  $100^\circ/s$ . *Solid lines* indicate predictions of the model and *filled circles* experimental results. The *bars* give standard errors of the experimental results. Note that the scale for the horizontal component is increased by a factor of 2 in both columns. The *dotted grid* always indicates steps of  $4^\circ/s$



equivalent to changing the zero or reference point of this transfer function.

To make the model consistent with the observed behavior during centrifugation, we added an additional high-pass filter in the linear velocity response path. While this element was not necessary to reproduce the responses during OVAR, it extended the applicability of the model with the same set of parameters to other paradigms such as centrifugation. For this paradigm it prevented the model from displaying a continuous nystagmus caused by the sustained acceleration, a feature not observed in the experiments (Curthoys et al. 1998).

### Model predictions

The model successfully reproduced most three-dimensional eye-velocity features for OVAR. To ensure a close correspondence between the simulated and the experimental conditions, we modeled vestibulo-ocular responses for 60 s and used the same analysis methods as described for the experimental data. The values given below, as well as the velocity offsets and modulation amplitudes shown in Fig. 5, correspond to simulations of OVAR with an acceleration of  $100^\circ/\text{s}^2$ , a constant velocity of  $100^\circ/\text{s}$ , and the model parameters given in Appendix C. To ensure that modeled and experimental data are analyzed in the same way, the eye velocity was modeled for 60 s after the end of the acceleration, and the last 25 s of that interval were used for the fitting procedure. Specifically, the model shows:

1. An increase in the horizontal, vertical, and torsional velocity modulation amplitudes with increasing tilt angle, which corresponds well in size with the experimental data from our experiments (Fig. 5, right column). The model indicates that the mechanisms generating the horizontal eye-velocity modulation are different from the ones generating the vertical/torsional modulations: while the horizontal modulation is determined by  $k_a$ , the vertical/torsional modulation amplitudes are controlled by  $k_{f\omega}$ .
2. A small horizontal velocity bias, which increases with increasing tilt angle (Fig. 5, left column) and is mainly caused by the coupling of the otolith-based head velocity estimates through  $k_{f\omega}$  to the angular velocity loop. Our modification of the otolith transfer function also generated a small vertical velocity bias, which has been noted in experiments in humans as well as in monkeys (Harris and Barnes 1987; Angelaki and Hess 1996a), and which we also found for higher velocity rotations about an earth-horizontal axis.
3. A maximum velocity that is approximately independent of the tilt angle for the acceleration phase (“per-rotatory”: from  $47.8^\circ/\text{s}$  for rotations about an earth-vertical axis to  $50.3^\circ/\text{s}$  for OVAR about an earth-horizontal axis), and that decreases with increasing tilt for deceleration (“postrotatory”: from  $50.3^\circ/\text{s}$  for rotations about an earth-vertical axis to  $39.0^\circ/\text{s}$  for

OVAR about an earth-horizontal axis). This corresponds to the decrease observed in our experiments, as well as in other studies in cats (Harris 1987) and monkeys (Raphan et al. 1981). As suggested by Raphan and Cohen, the tilt dependence of the maximum velocity during deceleration corresponded approximately to the per-rotatory horizontal velocity offset induced by OVAR rotation.

4. For high-velocity OVAR, the model predicted an interesting effect, not yet observed experimentally: when a subject is rotated at  $150^\circ/\text{s}$ , the horizontal eye velocity decreases to zero after about 2 min (Stockwell et al. 1972; Darlot et al. 1988). At this point all experiments have been terminated. But the model predicts that the eye velocity will rise again after the 2-min mark, to show a final, sustained offset that is about  $3^\circ/\text{s}$  larger than at the 2-min mark.

While our extended model successfully predicts horizontal, vertical, and torsional eye-velocity features for a large number of paradigms and a wide range of parameters, it also has clear limitations:

1. The phases of the velocity modulations are predicted to be approximately independent of the tilt angle, which contradicts the experimental data.
2. The model predicts a time constant of the horizontal velocity that is independent of the tilt angle, for accelerations and for decelerations. While the experimental values for acceleration are ambiguous, this prediction clearly disagrees with the experimental data for deceleration.
3. It also does not include eye position effects, which are especially noticeable in the torsional component (Fig. 2A).

---

## Discussion

### Experimental findings

In this study we have for the first time systematically investigated the effects of dynamic otolith input, elicited by OVAR, on three-dimensional eye movements in humans. In cats (Harris 1987; Darlot and Denise 1988), monkeys Raphan et al. 1981; Angelaki and Hess 1996a), and rats (Hess and Dieringer 1990), such a stimulus elicits eye movements with a velocity offset that compensates fairly well for the movement of the body in space. In humans, however, the compensatory eye velocity is dramatically smaller. Our small values for the horizontal and vertical offsets as well as for the modulation amplitudes agree with the values from another study in humans that used search coils to measure eye movements (Harris and Barnes 1987). Two other studies that used electro-oculography reported similar offsets but larger modulation values (Darlot et al. 1988; Furman et al. 1992). All these other studies in humans were performed

with a rotational velocity of 60°/s and with tilt angles only up to 30°.

This small effect of dynamic otolith input onto eye velocity is consistent with the results from other experiments that tested otolith-canal interactions: investigations of postrotatory tilt after deceleration from a constant velocity rotation have shown that in humans the change in the otolith input has no direct effect on the axis of eye velocity, and horizontal eye movements stay horizontal even after the tilt (Fetter et al. 1996). In monkeys, on the other hand, the changed otolith input transforms purely horizontal eye movements into combined horizontal and – depending on the direction of the tilt – vertical or torsional movements (Angelaki and Hess 1994). Similarly, the modification of the eye velocity responses by the linear acceleration components during rotations on a centrifuge is significantly larger in monkeys (Merfeld and Young 1995) than in humans (Curthoys et al. 1998, 1999).

We were surprised to find that the additional otolith input during OVAR does not help to prolong the canal-induced VOR, but shortens it. This result is supported by the short time constant during yaw rotation about an earth-horizontal axis (Tweed et al. 1994) and is similar to the reduction of the time constant during postrotatory tilt (Fetter et al. 1992). However, while in those experiments otoliths and canals gave conflicting information, in our paradigm both sensory systems indicated movement during the acceleration and deceleration phase.

In the per-rotary steady state situation, the dynamic otolith input provides ambiguous information: the direction of the gravito-inertial pull is the same, whether it is elicited by off-vertical axis rotation or by *counter-rotation out on the arm of a centrifuge*. For the latter paradigm, it is necessary to have a centrifuge with a rotator mounted out on the arm of the centrifuge. If the eccentric rotator is counter-rotating such that the orientation of the subject with respect to space remains constant, the direction of the otolith input is equivalent to the one experienced during OVAR. Only the total magnitude of the gravito-inertial force is slightly elevated. To determine which stimulus interpretation is chosen by the (central nervous system) CNS, it would be necessary to record binocular eye movements with controlled target distance – something that was not done in our experiments. However, small horizontal eye position modulations (Fig. 2A), as well as the verbal descriptions of the perceived movement during OVAR, indicate that this interpretation of the stimulus plays only a minor role.

Comparisons of our results for the horizontal and vertical velocity modulation phases with other studies are complicated by different conventions being used in different studies. Using our definitions, the studies by Harris and Barnes (1987) reported a phase lead of about 20° for the modulation of the horizontal eye velocity and of 104° for the modulation of the vertical eye velocity (rotations to the left). Darlot et al. reported a phase lead of 120° for the horizontal component and no phase shift for the vertical component (Darlot et al. 1988). The

phase values in our study (at 30° tilt a 10° phase lag for the horizontal eye velocity, and a 35° phase lead for the vertical component) are not consistent with either of these values. This difference might be partly due to the higher velocity used in our study.

The sometimes large intersubject variability may be related to the highly nauseous and disorienting nature of the paradigm. During a standard vestibular test, for example, a rotation about an earth-vertical axis, the vestibular system experiences an unambiguous input and can produce a clear, well-defined response. During OVAR, in contrast, the otolith system indicates sustained movement, while the semicircular canals indicate no movement at all. It is probably this conflict that causes about half the subjects to feel nauseous and that occasionally induced vomiting during or immediately after the OVAR rotation.

## Model

While the original model by Merfeld was successfully used to simulate the eye velocity responses for a number of paradigms, it could not match our experimental data for rotations about axes that were tilted by more than 45°: While the Merfeld model indicated vertical/torsional eye-velocity modulations that decrease for tilt angles above 45° and vanish at 90°, our data clearly disagree with this prediction (Fig. 5, experimental data).

We found that the simplest way to reproduce the observed vertical/torsional velocity modulations at large tilt angles was to add a constant external force to the otolith transfer functions  $S_{oto}$ , such that the otoliths are in equilibrium when the head is upright. This constant external force does not have to correspond to an actual physical force: addition of a constant force is equivalent to a simple shift in the reference or zero point of the otolith transfer function.

The idea of an additional external force was based on a suggestion by Dai et al. (1989): Dai assumed that the otolith signals are modified peripherally by a constant pitch-shear force along the utricular plane. This would balance the gravitational pull on the otoconia when the head is in a natural upright position, with the otoliths tilted approximately 30° nose up. They were able to show that this assumption can help to explain the errors in the estimation of the subjective vertical during roll tilts for all roll angles and under different  $g$ -levels. Combining this assumption with the Merfeld model, we obtained a model that correctly predicted the three-dimensional eye-velocity characteristics.<sup>1</sup>

The vertical/torsional velocity modulations could be generated by adding the external force only to the actual otolith transfer function  $S_{oto}$ . The modulation compo-

<sup>1</sup> Application of the model to other otolith-canal interactions such as rotation out on the arm of a centrifuge, postrotatory tilt, and “pitching while rotating” showed that our extended model was able to reproduce the observed three-dimensional eye movements correctly also for these paradigms.

nents were maintained if the force was also added to the internal representation  $\hat{S}_{oto}$ , which makes the model consistent with the idea of internal representations of the peripheral transfer functions.

The addition of an additional force to the otolith transfer function leads to only subtle changes in the peripheral otolith signals. For example, it implies a shift of the on-directions of peripheral otolith neurons as a function of the magnitude of the linear acceleration used to determine these on-directions. It also predicts an increase in the firing rate of neurons with forward on-directions on tilting the subject to the left or right side. So far no electrophysiological investigation has been made to explore these effects.

The introduction of this additional force component on the otoliths also induced a small vertical velocity offset in the model. Such an offset has been reported previously by Harris and Barnes (1987). Although not commented upon, it is also visible in the monkey data presented by Angelaki and Hess (1996a; Fig. 1, top). It also shows up in our data for high-velocity rotations about an earth-horizontal axis.

The model predicts that the horizontal eye-velocity modulation has a different source from the vertical and torsional modulation components. This prediction of the model could be tested experimentally: changing the fixation distance of an (imagined) target should change the horizontal modulation component, which uses the fixation distance-dependent path of the linear VOR (LVOR). The vertical/torsional components, however, should be unaffected, since they are mediated through the angular velocity pathways.

The model is consistent with the hypothesis by Raphan and Schnabolk (1988) that otolith signals are processed in a “head velocity estimator” before activating the velocity-storage integrator. This corresponds to the structure of our model, where the head velocity is estimated by comparing the expected direction of the gravito-inertial force with the perceived direction. This separation of head velocity estimation and velocity storage is also visible in other experimental data: in cerebellar patients the velocity storage is still intact, but the efficacy of the head velocity estimation is reduced (Anastasopoulos et al. 1990). Similarly, rhesus monkeys who have their nodulus and the central uvula removed surgically show an increase in the horizontal velocity storage, while the horizontal velocity offset is abolished (Angelaki and Hess 1995b).

Finally, the model challenges the suggestion that a neural circuit behaving as a low-pass filter should exist in the otolith-ocular pathway (Darlot et al. 1988). This suggestion was based on the finding that the eye velocity bias induced by OVAR is eliminated after 2 min of high-velocity rotation (Stockwell et al. 1972; Darlot et al. 1988). In contrast, our model suggests that the velocity bias is not eliminated. Instead the vestibular adaptation mechanism that causes the secondary nystagmus may induce a transient cancellation of the velocity bias, but the bias reappears again for longer duration OVAR.

**Acknowledgements** This study was supported by the Deutsche Forschungsgemeinschaft, SFB 307-A10. We want to thank Dr. Straumann and Dr. B. J. M. Hess for valuable comments on the manuscripts, and we are especially grateful to Dr. D. Tweed for the extensive discussions as well as for the permission to reanalyze data from his earlier study.

---

## Appendix A

### Vertical phase shifts

The phase of the turntable when rotating to the left with an angular velocity of  $\omega$  is given by “ $\omega t$ ”. Let the vertical eye-velocity or -position response have a phase delay of “ $\delta_L$ ”, so that the phase of the vertical response is given by  $\omega t + \delta_L$ . When the turntable rotates in the *opposite* direction, i.e., to the right, its position is given by “ $-\omega t$ ”. If the phase delay for rotations to the right is “ $\delta_R$ ”, the total phase of the vertical response is  $-\omega t + \delta_R$ . In a symmetrical subject, the vertical eye-movement response will be equivalent for rotations to the left and to the right. Therefore the following equation must hold:

$$-\omega t + \delta_R = \omega t + \delta_L$$

Since a phase shift of  $180^\circ$  inverts the sign of the phase, i.e.,  $-\omega t = \omega t + 180^\circ$ , we obtain  $\delta_R = \delta_L + 180^\circ$ . This explains the phase shift of approximately  $180^\circ$  in Fig. 3.

---

## Appendix B

### Dispersion

“Dispersion” is the spherical analog of variance (Watson 1983). It is a measure based on statistics of spheres that quantifies how well directions cluster in space, and can vary between 0 and 1. This is necessary because phase values of  $1^\circ$  and  $359^\circ$  differ by only  $2^\circ$ , and not by  $358^\circ$ . The dispersion-factor handles this circularity of the phase correctly, whereas the standard deviation, calculated in the regular fashion, would yield a wrong result.

Since many researchers are not used to working with dispersions, we converted the dispersion-values to standard deviations by using a reference table. The table was generated by taking a distribution of 40,000 random phase values with a given standard deviation, ignoring the circularity of the phase. Then the dispersion was calculated for this phase distribution. This procedure was repeated for phase samples with standard deviations between  $0.5^\circ$  and  $200^\circ$ , in  $0.5^\circ$  steps.

A dispersion value of zero would indicate that all vectors point in the same direction; a value of 0.01/0.1/0.25 would correspond to normal distribution of phases with a standard deviation of approximately  $8^\circ/27^\circ/44^\circ$ . A value of 1 would indicate that the phase values are distributed evenly between  $0^\circ$  and  $360^\circ$ .

---

## Appendix C

### Description of the Simulink model

The model is constructed around two negative feedback loops, indicated in Fig. 4 by dashed arrows, the lower loop processing the angular velocity signals measured by the semicircular canals and the upper loop the signals from the otoliths. The transfer function describing the transduction properties of the semicircular canals is the diagonal  $3 \times 3$  matrix  $S_{scc}$ , where the diagonal elements are given by:

$$scc(s) = \frac{\tau_a \tau_d s^2}{(\tau_a s + 1)(\tau_d s + 1)}$$

where  $\tau_d$  is the dominant time constant and  $\tau_a$  the adaptive time constant, respectively. Internal estimates of the vestibular transfer functions implement the model assumption that the brain “knows” how the original signal was transformed by the semicircular canals. In Fig. 4 “ $\wedge$ ” indicates internal estimates of the respective parameters. For the internal estimate of the canal transfer function,  $\hat{S}_{\text{acc}}(s)$ , the adaptive time constant can be discarded without affecting the model output, and the diagonal elements are reduced to:

$$\frac{\tau_d s}{(\tau_d s + 1)}$$

(Merfeld 1995).

Increasing the feedback parameter  $k_\omega$  not only increases the maximum velocity elicited by acceleration and the time constant of its decay, it also increases the offset velocity.

A similar loop is implemented for the signal coming from the otoliths (Fig. 4, upper dashed arrow). There  $k_a$  determines the gain for the linear vestibulo-ocular reflex (LVOR), and mainly influences the horizontal eye-velocity modulation.

The second important concept of the model is the head-velocity estimation based on the otolith signals, which connects the otoliths and the canals. The neural signal coming from the otolith afferents corresponds to the gravito-inertial force  $f$ , which is the difference between gravity  $g$  and linear acceleration  $a$ , filtered by the otolith transfer function  $S_{\text{oto}}$  ( $S_{\text{oto}}$  is given by the identity matrix plus a constant force along the dorsoventral axis). This signal is compared with the corresponding estimated value,  $\hat{S}_{\text{oto}} \cdot \hat{f}$ . Any directional mismatch between the two signals is interpreted as a head rotation, and is calculated by taking the cross-product of the two (indicated by “ $\times$ ” in Fig. 4). In the model the mismatch is caused by the lag between the expected orientation of the gravito-inertial force and the sensed orientation. It is the origin of the horizontal eye-velocity offset generated by the model, as well as the vertical/torsional velocity modulations for larger tilt angles. This estimate of the head rotation is coupled to the velocity-storage loop with the gain  $k_{f_0}$ . The direct coupling of the cross product with the gain factor  $k_f$  to the estimate of the direction of gravity ( $\wedge g$ ) is necessary, because changes in the perceived direction of gravity show different dynamics from the eye velocity, e.g., during angular acceleration out on the arm of a centrifuge.

The model does not include or predict any eye-position effects. To avoid the gaze dependence of the LVOR, we therefore assumed that the subject was always looking straight ahead. The effect of the fixation distance was included in the LVOR pathway by the term  $\hat{i} \times d^{-1}$  (Fig. 4), where “ $d^{-1}$ ” is a vector whose norm is the inverse of an imagined target distance and whose direction is aligned with the gaze direction.

We adjusted the four gain elements ( $k_\omega$ ,  $k_{f_0}$ ,  $k_a$ ,  $k_f$ ) such that the model output was close to the experimental findings. The model parameters had to stay within physiologically reasonable limits, as far as those limits are known. For example, the peripheral time constant for the decay of the eye-velocity signal had to lie between 6.5 s and 10 s (based on the mean response of primary afferent neurons in the squirrel monkey by Fernandez and Goldberg (1971)). By changing the model parameters, we then studied the effect of the different model elements on the output of the system. The following model parameters produced the best agreement with our experimental data:  $k_a = -1$ ,  $k_f = 10$ ,  $k_{f_0} = 1$ ,  $k_\omega = 1$ ,  $\tau_d^{\text{acc}} = 7$ ,  $\tau_a^{\text{acc}} = 190$ ,  $\tau_{\text{Integ}} = 2$ ,  $\tau_{\text{HighPass}} = 0.3$ ,  $d = 3$ . To run the simulation we used the variable step algorithm *ode45*, which is based on an explicit Runge-Kutta (4,5) formula (Dormand-Prince pair). *Initial step size* was set to  $1.0 \times 10^{-10}$  s, and the *maximum step size* was set to 0.1 s.

## References

- Anastasopoulos D, Haslwanter T, Fetter M, Dichgans J (1998) Smooth pursuit eye movements and otolith-ocular responses are differently impaired in cerebellar ataxia. *Brain* 121(8): 1497–1505
- Angelaki DE (1992a) Two-dimensional coding of linear acceleration and the angular velocity sensitivity of the otolith system. *Biol Cybern* 67:511–521
- Angelaki DE (1992b) Detection of rotating gravity signals. *Biol Cybern* 67:523–533
- Angelaki DE, Hess BJ (1994) Inertial representation of angular motion in the vestibular system of rhesus monkeys. I. Vestibulo-ocular reflex. *Neurophysiology* 71:1222–1249
- Angelaki DE, Hess BJ (1995a) Inertial representation of angular motion in the vestibular system of rhesus monkeys. II. Otolith-controlled transformation that depends on an intact cerebellar nodulus. *J Neurophysiol* 73:1729–1751
- Angelaki DE, Hess BJ (1995b) Lesion of the nodulus and ventral uvula abolish steady-state off-vertical axis otolith response. *J Neurophysiol* 73:1716–1720
- Angelaki DE, Hess BJ (1996a) Three-dimensional organization of otolith-ocular reflexes in rhesus monkeys. II. Inertial detection of angular velocity. *J Neurophysiol* 75:2425–2440
- Angelaki DE, Hess BJ (1996b) Three-dimensional organization of otolith-ocular reflexes in rhesus monkeys. I. Linear acceleration responses during off-vertical axis rotation. *J Neurophysiol* 75:2405–2424
- Bechert K, Koenig E (1996) A search coil system with automatic field stabilization, calibration, and geometric processing for eye movement recording in humans. *Neuro-ophthalmology* 16:163–170
- Curthoys IS, Haslwanter T, Black RA, Burgess AM, Halmagyi GM, Topple AN, Todd MJ (1998) Off-center yaw rotation: effect of naso-occipital linear acceleration on the nystagmus response of normal human subjects and patients after unilateral vestibular loss. *Exp Brain Res* 123:425–438
- Curthoys IS, Halmagyi GM, Haslwanter T, Burgess AM, Black RA, Topple A (1999) Human three dimensional eye movements in response to interaural linear acceleration during off center yaw rotation on a centrifuge. *Arch Ital Biol* 137:44–45
- Dai MJ, Curthoys IS, Halmagyi GM (1989) A model of otolith stimulation. *Biol Cybern* 60:185–194
- Darlot C, Denise P (1988) Nystagmus induced by off-vertical rotation axis in the cat. *Exp Brain Res* 73:78–90
- Darlot C, Denise P, Droulez J, Cohen B, Berthoz A (1988) Eye movements induced by off-vertical axis rotation (OVAR) at small angles of tilt. *Exp Brain Res* 73:91–105
- Fernandez C, Goldberg JM (1971) Physiology of peripheral neurons innervating semicircular canals of the squirrel monkey. II. Response to sinusoidal stimulation and dynamics of peripheral vestibular system. *J Neurophysiol* 34:661–675
- Fetter M, Tweed D, Hermann W, Wohland-Braun B, Koenig E (1992) The influence of head position and head reorientation on the axis of eye rotation and the vestibular time constant during postrotatory nystagmus. *Exp Brain Res* 91:121–128
- Fetter M, Heimberger J, Black RA, Hermann W, Sievering F, Dichgans J (1996) Otolith-semicircular canal interaction during postrotatory nystagmus in humans. *Exp Brain Res* 108: 463–472
- Furman JM, Schor RH, Schumann TL (1992) Off-vertical axis rotation: a test of the otolith-ocular reflex. *Ann Otol Rhinol Laryngol* 101:643–650
- Glasauer S, Merfeld DM (1997) Modeling three-dimensional vestibular responses during complex motion stimulation. In: Fetter M, Haslwanter T, Misslisch H, Tweed D (eds) *Three-dimensional kinematics of eye, head and limb movements*. Harwood Academic, Amsterdam, pp 387–398
- Hain TC (1986) A model of the nystagmus induced by off-vertical axis rotation. *Biol Cybern* 54:337–350
- Harris LR (1987) Vestibular and optokinetic eye movements evoked in the cat by rotation about a tilted axis. *Exp Brain Res* 66:522–532
- Harris LR, Barnes GR (1987) Orientation of vestibular nystagmus is modified by head tilt. In: Graham MD, Kemink JL (eds) *The vestibular system: neurophysiologic and clinical research*. Raven, New York, pp 539–548
- Hess BJM (1992) Three-dimensional head angular velocity detection from otolith afferent signals. *Biol Cybern* 67:323–333

- Hess BJ, Dieringer N (1990) Spatial organization of the maculo-ocular reflex of the rat: responses during off-vertical axis rotation. *Eur J Neurosci* 2:909–919
- Holden JR, Wearne SL, Curthoys IS (1992) A fast, portable desaccading program. *J Vestib Res* 2:175–179
- Merfeld DM (1995a) Modeling the vestibulo-ocular reflex of the squirrel monkey during eccentric rotation and roll tilt. *Exp Brain Res* 106:123–134
- Merfeld DM, Young LR (1995) The vestibulo-ocular reflex of the squirrel monkey during eccentric rotation and roll tilt. *Exp Brain Res* 106:111–122
- Merfeld D, Young LR, Oman CM, Shelhamer M (1993) A multi-dimensional model of the effect of gravity on the spatial orientation of the monkey. *J Vestib Res* 3:141–161
- Merfeld DM, Zupan L, Peterka RJ (1999) Humans use internal models to estimate gravity and linear acceleration. *Nature* 398:615–618
- Press WH, Teukolsky SA, Vetterling WT, Flannery SA (1992) *Numerical recipes in C*, 2nd edn. Cambridge University Press, Cambridge
- Raphan T, Schnabolk C (1988) Modeling slow phase velocity generation during off-vertical axis rotation. *Ann NY Acad Sci* 545:29–50
- Raphan T, Cohen B, Henn V (1981) Effects of gravity on rotatory nystagmus in monkeys. *Ann NY Acad Sci* 374:44–55
- Savitzky A, Golay MJ (1964) Smoothing and differentiation of data by simplified least squares procedures. *Anal Chem* 36:1627–1639
- Schnabolk C, Raphan T (1992) Modeling 3-D slow phase velocity estimation during off-vertical-axis rotation (OVAR). *J Vestib Res* 3:123–139
- Stockwell CW, Guedry FE, Turnipseed GT, Graybiel A (1972) The nystagmus response during rotation about a tilted axis. *Minerva Otorhinolaryngologica* 22:229–235
- Tweed D, Cadera W, Vilis T (1990) Computing three-dimensional eye position quaternions and eye velocity from search coil signals. *Vision Res* 30:97–110
- Tweed D, Fetter M, Sievering D, Misslisch H, Koenig E (1994) Rotational kinematics of the human vestibuloocular reflex. II. Velocity steps. *J Neurophysiol* 72:2480–2489
- Watson GS (1983) *Statistics on spheres*. Wiley, New York